Unsteady Compressible Heat Transfer in Supercritical Fluids

Leonardo S. de B. Alves, leonardo.alves@mec.uff.br

Laboratório de Mecânica Teórica e Aplicada, Departamento de Engenharia Mecânica, Universidade Federal Fluminense, Rua Passo da Pátria 156, Bloco E, Sala 216, Niterói, RJ 24210-240, Brazil.

Abstract. *Highly compressible fluids constrained by solid walls undergo a rapid increase in bulk temperature T_b due to the propagation and reflection of pressure waves. The particular case of supercritical fluids under microgravity has a classical thermodynamic model given by the traditional heat equation with an addition source term containing the bulk temperature time derivative. An approximate solution for the bulk temperature generated with Dirichlet boundary conditions, obtained when this model was first proposed, naturally includes an expression for the characteristic time of this compressible heat transfer phenomenon, which has been called the piston effect relaxation time t_{PE}. It is defined as $t_{PE} = t_D/(\gamma - 1)^2$, where t_D is the thermal diffusion relaxation time and γ is the ratio between specific heats. The approximate solution can also be used to estimate this characteristic time through $T_b(t_E)/T_1 \simeq 0.99$, a criteria motivated by classical boundary-layer theory, where t_E is the piston effect relaxation time estimate and T_1 is the bulk temperature steady-state. However, such a calculation yields $t_E/t_{PE} \simeq 3182.1$, which is more than three orders of magnitude higher than expected. Motivated by this finding, the present paper derives the exact analytical solution for the same thermodynamic model and extracts its characteristic times. They show that the correct piston effect relaxation time should be $t_{PE} = t_D/\gamma$ instead, which is rigorously satisfied by the exact solution when Dirichlet boundary conditions are imposed. On the other hand, the fast thermal boundary-layer expansion responsible for the piston effect is inhibited when heating is imposed through either Neumann or Cauchy boundary conditions, leading to $t_E \gg t_{PE}$.*

Keywords: *Piston Effect, Relaxation Times, Compressible Flows, Supercritical Fluids, Integral Transforms*

1. INTRODUCTION

All fluids are subject to an universal divergence of their thermodynamic properties near their critical points. This phenomenon should lead to a critical slowing-down of temperature equilibration due to a diverging thermal diffusion relaxation time $t_D = l^2/\alpha$, where l is a characteristic length and $\alpha = k/(\rho C_P)$ is the thermal diffusivity. The latter vanishes near the critical point because specific heat at constant pressure C_P diverges faster than thermal conductivity k while density ρ remains bounded. However, very fast temperature equilibration was still observed in enclosed samples on ground-based experiments (Dahl and Moldover, 1972). Gravity induced buoyancy was assumed responsible for this effect until 25 years ago, when low gravity experiments in orbiting rockets yielded similar results (Nitsche and Straub, 1987). Such a critical speeding-up was explained from a thermodynamic standpoint (Boukari *et al.*, 1990; Onuki *et al.*, 1990) and using the Navier-Stokes equations (Zappoli *et al.*, 1990) soon afterwards. It is caused by the ability of small temperature perturbations to create severe compression in near-critical fluids, which, in turn, generates thermo-acoustic waves. When entrapped within cavity walls, their propagation and reflection induces a rapid heating of the entire fluid, resulting in a homogeneous increase of its bulk temperature. This phenomenon, known today as piston effect, has been validated by theoretical, numerical and experimental studies (Zappoli, 2003; Barmatz *et al.*, 2007; Carlès, 2010).

The thermodynamic model proposed (Boukari *et al.*, 1990; Onuki *et al.*, 1990) leads to the one-dimensional unsteady heat conduction equation with a source term proportional to the bulk temperature time derivative. This source term models the adiabatic compression mechanism responsible for the piston effect. It becomes dominant whenever $\gamma \gg 1$, which occurs close to the critical point. On the other hand, it vanishes in the incompressible limit, where $\gamma = 1$. In order to reproduce a then recent microgravity experiment (Nitsche and Straub, 1987), Onuki and Ferrell (1990) considered a fluid initially at T_0 and bounded by solid walls, whose temperatures were suddenly raised to T_1. They used an approximate

Fourier transformation procedure to obtain

$$T_b(t) = T_0 + \Delta T \left(1 - \exp\left[\frac{t}{t_{PE}}\right] \operatorname{erfc}\left[\sqrt{\frac{t}{t_{PE}}}\right]\right) , \tag{1}$$

for the bulk temperature, where $\Delta T = T_1 - T_0$, t_{PE} is the piston effect relation time defined as

$$t_{PE} = \frac{t_D}{(\gamma - 1)^2} , \tag{2}$$

$\gamma = C_P/C_V$ and C_V is the specific heat at constant volume. Although these original studies imposed steady heating at the boundaries, they were extended towards pulsed (Ferrell and Hao, 1993) and unsteady (Garrabos *et al.*, 1998) heating as well. A similar solution procedure was employed in these additional studies, which also led to expression (2) for t_{PE}. This model was extended to include two dimensions as well as curvature effects, introduced by cylindrical container walls (Carlès *et al.*, 2005). The authors employed Separation of Variables and Laplace transform with numerical inversion to solve the governing equations. However, they propose expression $t_{PE} = t_D/\gamma^2$ instead of expression (2), with t_D based on the cylinder diameter as characteristic length. It is interesting to note that this new expression implies $t_{PE} < t_D$ for $\gamma > 1$, in contradiction with $\gamma > 2$ for expression (2). In fact, the latter implies that $t_{PE} > t_D$ for $1 < \gamma < 2$, which has not been observed in thermo-acoustic simulations and experiments under atmospheric conditions (Huang and Bau, 1997). This is not the only contradiction associated with expression (2). Solution (1) can be used to generate an estimate t_E for the piston effect relaxation time t_{PE} from a criterion such as $T_b(t_E)/T_1 \simeq 0.99$, which is based on classical boundary-layer theory (Schlichting, 1986). In doing so, one finds $t_E/t_{PE} \simeq 3182.1$. Such a number is more than three orders of magnitude higher than expected, indicating a serious discrepancy between expression (2) and the very same solution that defines it, given by bulk temperature approximation (1).

In the present paper, we focus on the same thermodynamic model for the piston effect to derive its exact analytical solution, i.e., without resorting to any approximations whatsoever. Furthermore, we utilize an eigenvalue analysis of this solution to extract its temperature relaxation times, demonstrating that only two different characteristic times exist but expression (2) is not among them. This discovery is generalized to several different thermal boundary conditions. The exact solution is obtained with a generalized version (Cotta, 1993) of the classical integral transform technique (Özisik, 1993), coupled with a standard filtering technique (Mikhailov and Özisik, 1984) and the matrix exponential function (Moler and Loan, 2003), where the eigenvalues are computed symbolically using *Mathematica* (Wolfram, 2003). This generalized integral transform technique has been successfully used in the literature to simulate natural convection in porous media (de B. Alves and Cotta, 2000), nonlinear convection-diffusion flows (de B. Alves *et al.*, 2001), Rayleigh-Benard instability in porous media (de B. Alves *et al.*, 2002), diffusion problems in irregular domains (Sphaier and Cotta, 2002), magnetohydrodynamics flow and heat transfer (Lima *et al.*, 2007), atmospheric pollutant dispersion (Almeida *et al.*, 2008), heat and mass transfer in adsorbed gas storage (Hirata *et al.*, 2009), convective heat transfer within wavy walls (Castellões *et al.*, 2010) and conjugate heat transfer using a single domain formulation (Knupp *et al.*, 2012).

2. MATHEMATICAL MODEL

The classical thermodynamic model for unsteady compressible heat transfer in a cavity containing a supercritical fluid under microgravity conditions is governed by a dimensionless equation for temperature in the form

$$\frac{\partial \top}{\partial \tau} - \left(1 - \frac{1}{\gamma}\right) \frac{d}{d\tau} \left(\int_0^1 \top \, d\xi \right) = \frac{\partial^2 \top}{\partial \xi^2} \quad , \tag{3}$$

which is subject to initial and boundary conditions

$$\top(\xi, 0) = 0 \quad , \quad - \left.\frac{\partial \top}{\partial \xi}\right|_{\xi=0} + \mathcal{L}_1 \top(0, \tau) = \mathcal{L}_2 \quad \text{and} \quad \left.\frac{\partial \top}{\partial \xi}\right|_{\xi=1} + \mathcal{R}_1 \top(1, \tau) = \mathcal{R}_2 \quad , \tag{4}$$

where $\mathcal{L}_1$, $\mathcal{L}_2$, $\mathcal{R}_1$ and $\mathcal{R}_2$ are parameters that define all nine possible combinations between Dirichlet, Neumann and Robin boundary conditions. These equations are based on dimensionless variables

$$\tau = \frac{t}{t_D} \quad , \quad \xi = \frac{x}{l} \quad \text{and} \quad \top = \left(\frac{\mathcal{L}_1^* + \mathcal{R}_1^* + \mathcal{L}_1^* \mathcal{R}_1^*}{\mathcal{L}_2^* \mathcal{R}_1^* - \mathcal{L}_1^* \mathcal{R}_2^*} \right) T - \left(\frac{\mathcal{L}_2^* + \mathcal{R}_2^* + \mathcal{L}_1^* \mathcal{R}_2^*}{\mathcal{L}_2^* \mathcal{R}_1^* - \mathcal{L}_1^* \mathcal{R}_2^*} \right) \quad , \tag{5}$$

with $\mathcal{L}_1^*$, $\mathcal{R}_1^*$, $\mathcal{L}_2^*$ and $\mathcal{R}_2^*$ referring to dimensional versions of their respective parameters without asterisks.

Three different sets of boundary conditions are going to be considered in the present study. They employ Dirichlet, Neumann and Robin boundary conditions on the left wall, but temperature is prescribed at T_0 on the right wall in all three cases. Such a choice leads to $\mathcal{R}_2 = 0$ and $\mathcal{R}_1 = \infty$. An additional constraint is imposed in the selection of $\mathcal{L}_1$ and $\mathcal{L}_2$ in order to guarantee that all boundary condition sets analyzed lead to the same steady-state solution, given by

$$\top(\xi, \infty) = 1 - \xi \quad , \tag{6}$$

which leads to the three boundary condition scenarios studies here and shown in Table 1. It should be noted that they are controlled by a single parameter named Bi and often referred to as Biot number.

Table 1. Three left wall boundaries analyzed in the present study using $\top(1, \tau) = 0$ at the right wall.

Boundary Type	Dirichlet	Neumann	Robin
Boundary Condition	$\top(0, \tau) = 1$	$-\left.\frac{\partial \top}{\partial \xi}\right\vert_{\xi=0} = 1$	$-\left.\frac{\partial \top}{\partial \xi}\right\vert_{\xi=0} + Bi\, \top(0, \tau) = 1 + Bi$
Boundary Constants	$\mathcal{L}_1 = \mathcal{L}_2 = \infty$	$\mathcal{L}_1 = 0 \;\&\; \mathcal{L}_2 = 1$	$\mathcal{L}_1 = Bi \;\&\; \mathcal{L}_2 = 1 + Bi$

3. SOLUTION PROCEDURE

3.1 Filtering

The first step towards a solution for the above system of equations is to separate steady and unsteady states (Mikhailov and Özisik, 1984). Although this is usually done to remove inhomogeneous boundary conditions and improve convergence rates, it also isolates the unsteady temperature features required in the present analysis. Hence, definition

$$\top(\xi, \tau) = \Theta(\xi) + \theta(\xi, \tau) \quad , \tag{7}$$

is employed here, where the steady-state filter is given by

$$\Theta(\xi) = \top(\xi, \infty) \quad , \tag{8}$$

already defined in (6). Furthermore, the particular case where $\mathcal{L}_1 = \mathcal{R}_1 = 0$ is excluded because steady-state $\Theta(\xi)$ either does not exist or is not unique. Substituting relation (7) into governing equation (3) leads to

$$\frac{\partial \theta}{\partial \tau} - \left(1 - \frac{1}{\gamma} \right) \frac{d}{d\tau} \int_0^1 \theta \, d\xi = \frac{\partial^2 \theta}{\partial \xi^2} \quad , \tag{9}$$

which governs the overall unsteady behavior $\theta(\xi, \tau)$ of the model problem (3). Its initial and boundary conditions are obtained in a similar way, substituting relation (7) into the respective conditions in (4), leading to

$$\theta(\xi, 0) = \xi - 1 \quad , \quad - \left.\frac{\partial \theta}{\partial \xi}\right|_{\xi=0} + Bi\, \theta(0, \tau) = 0 \quad \text{and} \quad \theta(1, \tau) = 0 \quad , \tag{10}$$

noting that they are also subject to the parameter restrictions specified in section 2.

3.2 Integral Transformation

Now, as a second step, spatial and temporal dependences of the model problem unsteady representation are separated by proposing a solution for equation (9) and boundary conditions in (10) with the form

$$\theta(\xi,\tau) \;=\; \sum_{i=1}^{\infty} \tilde{\psi}_i(\xi)\,\bar{\theta}_i(\tau) \quad , \tag{11}$$

where the basis function $\tilde{\psi}_i(\xi)$, responsible for the spatial dependence, is provided by the eigensystem

$$\frac{d^2\psi_i}{d\xi^2} \,+\, \beta_i^2\,\psi_i(\xi) \;=\; 0 \quad , \quad -\left.\frac{d\psi_i}{d\xi}\right|_{\xi=0} +\, Bi\,\psi_i(0) \;=\; 0 \quad \text{and} \quad \psi_i(1) \;=\; 0 \quad , \tag{12}$$

which is based on the model problem itself and yields the eigenfunctions

$$\psi_i(\xi) \;=\; \sin[\,\beta_i\,(1 \,-\, \xi)\,] \quad , \tag{13}$$

and transcendental equation

$$\beta_i\,\cos[\,\beta_i\,] + \,Bi\,\sin[\,\beta_i\,] = \,0 \quad , \tag{14}$$

that provides the eigenvalues, for $i = 1\,,\,2\,,\,\ldots\,,\,\infty$. Since these eigenfunctions are orthogonal, the integral transformed temperature coefficients $\bar{\theta}_i(\tau)$, responsible for the temporal dependence, can be defined according to relation

$$\bar{\theta}_i(\tau) \;=\; \int_0^1 \tilde{\psi}_i(\xi)\,\theta(\xi,\tau)\,d\xi \quad , \tag{15}$$

based on the above eigensystem (Özisik, 1993), where the norm

$$N_i \;=\; \int_0^1 \psi_i(\xi)^2\,d\xi \;=\; \frac{Bi \,+\, Bi^2 \,+\, \beta_i^2}{2\,(Bi^2 + \beta_i^2)} \quad , \tag{16}$$

is used to normalize the eigenfunctions for the basis function $\tilde{\psi}_i = \psi_i/\sqrt{N_i}$.

The third and final step involves the integral transformation of equation (9) to generate a system of equations that governs the behavior of the temperature coefficients. Multiplying this equation by $\tilde{\psi}_i$, integrating the result over the dimensionless cavity length and applying transformation (15) to the time derivative term, yields

$$\frac{d\bar{\theta}_i}{d\tau} - \eta_i\left(1 - \frac{1}{\gamma}\right)\frac{d\theta_b}{d\tau} \;=\; \int_0^1 \tilde{\psi}_i(\xi)\,\frac{\partial^2\theta}{\partial\xi^2}\,d\xi\,, \tag{17}$$

where integral transform coefficient and bulk temperature

$$\eta_i \;=\; \int_0^1 \tilde{\psi}_i(\xi)\,d\xi \;=\; \frac{1 - \cos[\,\beta_i\,]}{\beta_i\,\sqrt{N_i}} \quad \text{and} \quad \theta_b(\tau) \;=\; \int_0^1 \theta(\xi,\tau)\,d\xi \quad , \tag{18}$$

respectively, are defined for simplicity. Integrating the r.h.s. of equation (18) by parts, applying boundary conditions in (10) and (12), substituting the equation in (12) and then integral transform definition (15) into the result yields

$$\int_0^1 \tilde{\psi}_i(\xi)\,\frac{\partial^2\theta}{\partial\xi^2}\,d\xi \;=\; \int_0^1 \frac{d^2\tilde{\psi}_i}{d\xi^2}\,\theta(\xi,\tau)\,d\xi \;=\, -\,\beta_i^2\int_0^1 \tilde{\psi}_i(\xi)\,\theta(\xi,\tau)\,d\xi \;=\; -\,\beta_i^2\,\bar{\theta}_i(\tau) \quad , \tag{19}$$

which can be substituted into the r.h.s. of equation (17), with inverse definition (11) substituted into the non-transformed bulk temperature term of the same equation (Cotta, 1993), to generate

$$\sum_{j=1}^{\infty} A_{i,j}\,\frac{d\bar{\theta}_j}{d\tau} + \beta_i^2\,\bar{\theta}_i(\tau) = 0 \quad \text{where} \quad A_{i,j} = \delta_{i,j} - \left(1 - \frac{1}{\gamma}\right)\eta_i\,\eta_j \quad , \tag{20}$$

for $i = 1\,,\,2\,,\,\ldots\,,\,\infty$, which is subject to transformed initial condition

$$\bar{\theta}_i(0) = \int_0^1 (\xi - 1)\,\tilde{\psi}_i(\xi)\,d\xi = -(1 + Bi)\,\frac{\sin[\,\beta_i\,]}{\beta_i^2\,\sqrt{N_i}} = \frac{1 + Bi}{Bi}\,\frac{\cos[\,\beta_i\,]}{\beta_i\,\sqrt{N_i}} \quad , \tag{21}$$

obtained by transforming initial condition in (10), with $\delta_{i,j}$ representing the Kronecker delta. Two possibilities are given in (21) for both asymptotic limits of the Biot number, $Bi \to 0$ or $Bi \to \infty$, respectively. After solving system (20) with initial conditions (21) for the integral transformed temperature coefficients, the exact solution is obtained by combining them with relations (6) to (8) and (11) to generate

$$\top(\xi,\tau) = 1 - \xi + \sum_{i=1}^{\infty} \tilde{\psi}_i(\xi)\,\bar{\theta}_i(\tau) \quad , \tag{22}$$

where its bulk value, in agreement with the definition in (18), becomes

$$\top_b(\tau) = \int_0^1 \top(\xi,\tau)\,d\xi = \frac{1}{2} + \sum_{i=1}^{\infty} \eta_i\,\bar{\theta}_i(\tau) \quad , \tag{23}$$

which must be truncated. Because the eigensystem chosen in (12) belongs to the Sturm-Liouville class, the infinite summation series solution (22) is convergent (Cotta, 1993). Hence, it can be truncated at a high enough number, named N here, in order to guarantee a predetermined user-defined tolerance. Truncated version of system (20) and (21) is then solved analytically with a matrix exponential (Moler and Loan, 2003) using the software *Mathematica* (Wolfram, 2003).

4. RESULTS AND DISCUSSION

4.1 Dimensional Analysis

It is possible to decouple the time derivatives in equations (20) by introducing the new variable set

$$\bar{\theta}_i = \sum_{j=1}^{N} R_{i,j}\,\bar{q}_j \quad , \tag{24}$$

in equation (20) and multiplying the result by R^{-1} to generate

$$\lambda_i\,\frac{d\bar{q}_i}{d\tau} + \sum_{j=1}^{N} B_{i,j}\,\bar{q}_j(\tau) = 0 \quad , \tag{25}$$

for $i = 1\,,\,2\,,\,\ldots\,,\,\infty$, which, based on (21), is subject to initial conditions

$$\bar{q}_i(0) = \sum_{j=1}^{N} R^{-1}_{i,j}\,\bar{\theta}_j(0) \quad , \tag{26}$$

where λ_i and R are the eigenvalues and right eigenvector matrix of matrix A, respectively, and B is the resulting matrix transformation of β_i^2. It turns out R is independent of γ and, hence, so is matrix B.

Equations (25) to (26) still govern the entire unsteady response of the thermodynamic model, but now through $\bar{q}_i$ instead, which is just a linear combination of all $\bar{\theta}_i$. Hence, the characteristic times in equations (20) and (25) are the same. Assuming the dimensionless form chosen for temperature in (5) is correct, equation (25) explicitly shows that

τ/λ_i is the correct dimensionless time dictating the unsteady evolution of each $\bar{q}_i$, otherwise the order of magnitude of their respective time derivatives is not one. In other words, characteristic time scales should be $t_D\,\lambda_i$ instead of t_D used originally to define τ in (5). Calculating the eigenvalues of A in (20) using *Mathematica* (Wolfram, 2003), one obtains

$$\lambda_1 = \lambda_2 = \cdots = \lambda_{N-1} = 1 \quad \text{and} \quad \lambda_N = 1 - \left(1 - \tfrac{1}{\gamma}\right) \sum_{i=1}^{N} \eta_i^2 \quad , \tag{27}$$

which means only two different characteristic time scales exist in the truncated solution whenever $N \geqslant 2$. Furthermore,

$$\lim_{N\to\infty} \sum_{i=1}^{N} \eta_i^2 = 1\,, \tag{28}$$

so the last eigenvalue in (27) becomes $\lambda_\infty = 1/\gamma$ for the exact solution, as shown in Figure 5 (left). Hence, the two characteristic time scales associated with the original thermodynamic model, given by $t_D\,\lambda_i$, are

$$t_D \quad \text{and} \quad t_{PE} = \frac{t_D}{\gamma}\,, \tag{29}$$

where the former is the well-known thermal diffusion relaxation time and, therefore, the latter must be the piston effect relaxation time instead of (2), according to the exact solution of equations (3) to (4).

4.2 Boundary Effects

In order to analyze the effect of different thermal boundary conditions on the piston effect characteristic time, a baseline case is established. The first case, using a Dirichlet boundary condition on the left wall to heat the fluid, is considered for that purpose. Figure 1 (left) shows the local temperature profile at different times $t/t_{PE} = \gamma\,\tau$ for $\gamma = 50$. The strong thermal boundary-layer responsible for the adiabatic compression of the bulk fluid is quite clear at $t/t_{PE} \ll 1$, and so is the fast increase in the midpoint temperature. This latter effect is better visualized through the bulk temperature increase with time shown in Figure 1 (right) for different γ values. A curve representing the pure diffusion case, which can be obtained by imposing $\gamma = 1$, is also shown in order to illustrate the fast increase in bulk temperature as γ increases or, in other words, as the fluid gets closer to its critical point.

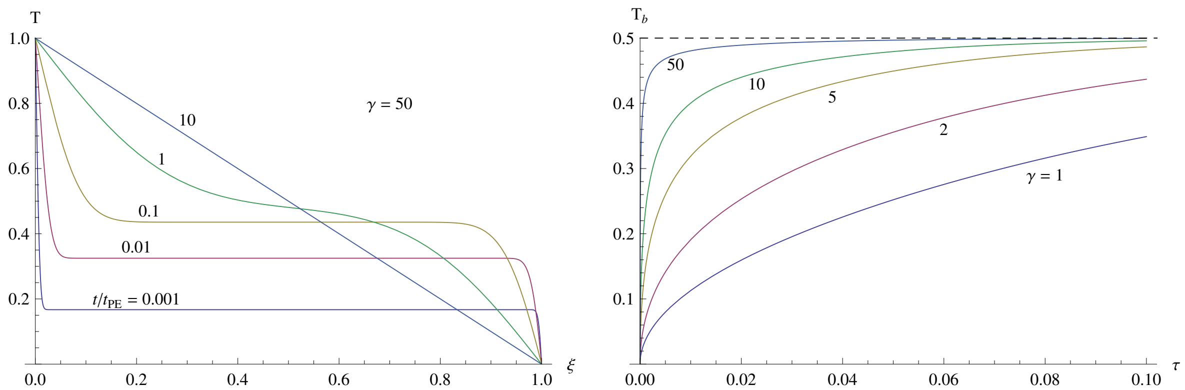

Figure 1. Local (left) and bulk (right) temperature profiles for a Dirichlet boundary condition at the left wall.

This behavior changes drastically when the left wall boundary condition is switched to a Neumann type. As shown in Figure 2, the thermal boundary-layer expansion (left) is much weaker when compared to the previous case with prescribed temperatures. In turn, the bulk temperature increase (right) is also severely weakened. Furthermore, an increase in γ leads to a reduction in piston effect relaxation time only up to $\gamma = 50$. Very little change is observed beyond this value for a simple reason. Fixing the left wall temperature gradient through a Neumann boundary condition restricts the thermal boundary-layer expansion and, hence, restricts the bulk temperature increase caused by the piston effect.

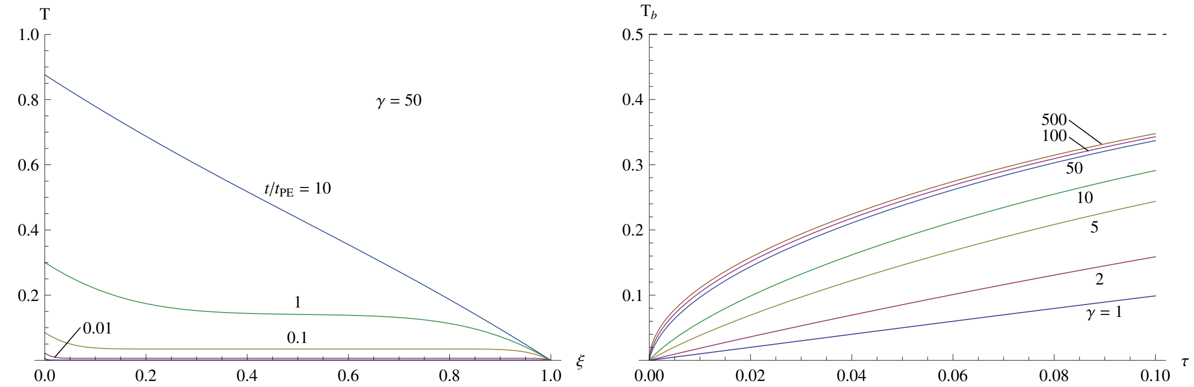

Figure 2. Local (left) and bulk (right) temperature profiles for a Neumann boundary condition at the left wall.

It is possible to analyze the fluid temperature behavior within an intermediate state between the previous two presented earlier by imposing a Robin boundary conditions at the left wall. Figure 3 shows local (left) and bulk (right) temperatures for this boundary condition with $Bi = 1$. Since the left wall temperature gradient is larger in this case, a slightly stronger bulk temperature increase can be observed. Nevertheless, it is still not as strong as the prescribed temperature case. Figure 4 shows the local (left) and bulk (right) temperature behavior for different Biot numbers, where the dashed lines represent the prescribed temperature and heat flux limiting cases. An increase in Biot number reduces the restriction imposed by the boundary condition to the thermal boundary layer expansion, allowing a greater bulk temperature expansion.

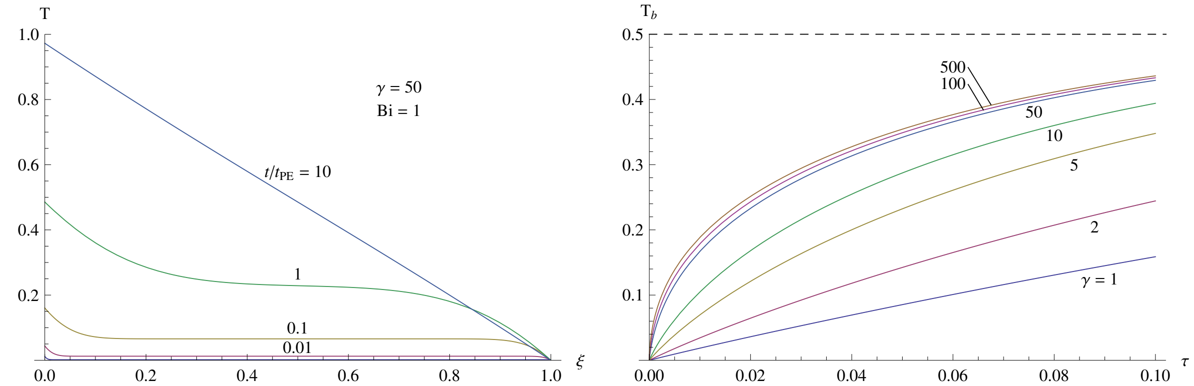

Figure 3. Local (left) and bulk (right) temperature profiles for a Robin boundary condition at the left wall.

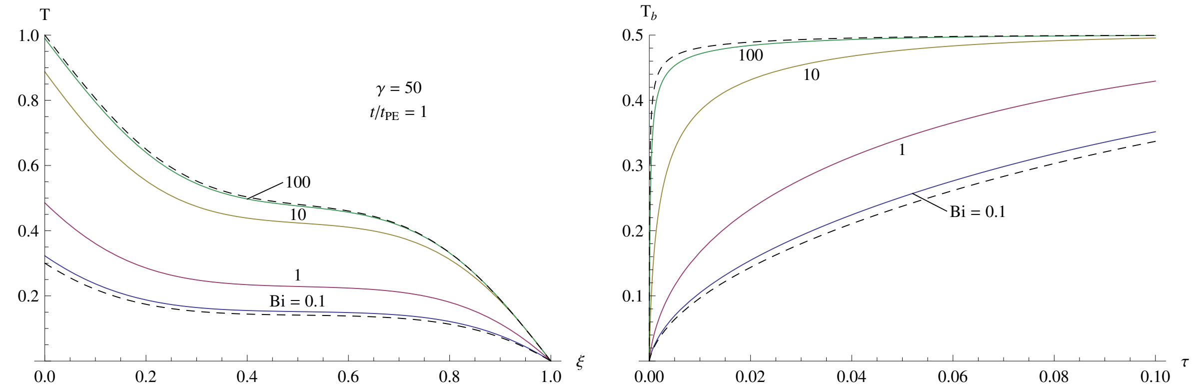

Figure 4. Biot number effect on the local (left) and bulk (right) temperature profiles for the Robin boundary condition.

The analytical (left) and estimated (right) piston effect relaxation times from the previous simulations are shown in Figure 5. The former (left) presents the error associated with analytical expression (29) for both $Bi = 0$ and ∞ cases whereas the latter (right) presents the characteristic time it takes the bulk temperature to reach 99% of its steady-state value for several Biot numbers, with the dashed line representing the theoretical value given by (29). Hence, theoretically derived expression (29) represents the correct piston effect relaxation time for high Biot numbers only.

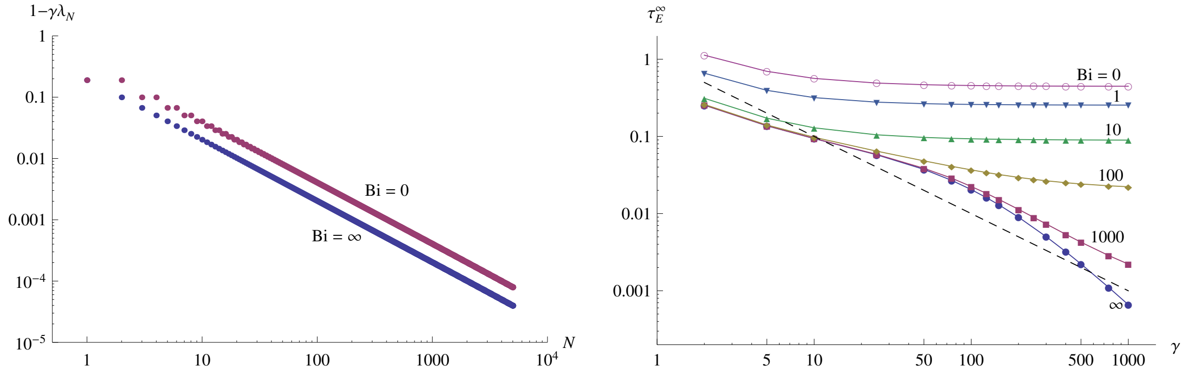

Figure 5. Analytical and estimated piston effect relaxation time for different Biot numbers.

5. CONCLUSIONS

An analytical solution for the thermodynamic model of compressible heat transfer was derived here for the first time. It lead to a new analytical expression for the piston effect relaxation time, which is qualitatively different from the classical expression available in the literature. This expression was shown to be consistent with the solution it was derived from, which is not the case with the classical expression. Furthermore, the influence of different thermal heating boundary conditions was evaluated. It was found that higher Biot numbers reduce the thermal boundary layer expansion responsible for the adiabatic compression that induces the piston effect, increasing the corresponding relaxation time.

6. REFERENCES

Almeida, G.L., Pimentel, L.C.G. and Cotta, R.M., 2008. “Integral transform solutions for atmospheric pollutant dispersion”. *Environmental Modeling and Assessment*, Vol. 13, No. 1, pp. 53–65.

Barmatz, M., Hahn, I., Lipa, J.A. and Duncan, R.V., 2007. “Critical phenomena in microgravity: Past, present and future”. *Reviews of Modern Physics*, Vol. 79, pp. 1–52.

Boukari, H., Shaumeyer, J.N., Briggs, M.E. and Gammon, R.W., 1990. “Critical speeding up in pure fluids”. *Physical Review A*, Vol. 41, No. 4, pp. 2260–2263.

Carlès, P., 2010. “A brief review of the thermophysical properties of supercritical fluids”. *The Journal of Supercritical Fluids*, Vol. 53, pp. 2–11.

Carlès, P., Zhong, F., Weilert, M. and Barmatz, M., 2005. “Temperature and density relaxation close to the liquid-gas critical point: An analytical solution for cylindrical cells”. *Physical Review E*, Vol. 71, p. 041201.

Castellões, F.V., Quaresma, J.N.N. and Cotta, R.M., 2010. “Convective heat ttransfer enhancement in low reynolds number flows with wavy walls”. *International Journal of Heat and Mass Transfer*, Vol. 53, No. 9, pp. 2022–2034.

Cotta, R.M., 1993. *Integral Transforms in Computational Heat and Fluid Flow*. CRC Press, Boca Raton, FL.

Dahl, D. and Moldover, M.R., 1972. “Thermal relaxation near the critical point”. *Physical Review A*, Vol. 6, No. 5, pp. 1915–1920.

de B. Alves, L.S. and Cotta, R.M., 2000. “Transient natural convection inside porous cavities:- hybrid numerical- analytical solution and mixed symbolic-numerical computation”. *Numerical Heat Transfer, Part A - Applications*, Vol. 38, No. 1, pp. 89–110.

de B. Alves, L.S., Cotta, R.M. and Mikhailov, M.D., 2001. “Covalidation of hybrid integral transforms and method of lines in nonlinear convection-diffusion with Mathematica”. *Journal of the Brazilian Society of Mechanical Sciences -*

RBCM, Vol. 23, No. 3, pp. 303–320.

de B. Alves, L.S., Cotta, R.M. and Pontes, J., 2002. "Stability analysis of natural convection in porous cavities through integral transforms". *International Journal of Heat and Mass Transfer*, Vol. 45, No. 6, pp. 1185–1195.

Ferrell, R.A. and Hao, H., 1993. "Adiabatic temperature changes in a one-component fluid near the liquid-vapor critical point". *Physical A*, Vol. 197, pp. 23–46.

Garrabos, Y., Bonetti, M., Beysens, D., Perrot, F., Fröhlich, T., Carlès, P. and Zappoli, B., 1998. "Relaxation of a supercritical fluid after a heat pulse in the absence of gravity effects: Theory and experiments". *Physical Review E*, Vol. 57, No. 5, pp. 5665–5681.

Hirata, S.C., Couto, P., Lara, L.G. and Cotta, R.M., 2009. "Modeling and hybrid simulation of slow discharge process of adsorbed methane tanks". *International Journal of Thermal Sciences*, Vol. 48, No. 6, pp. 1176–1183.

Huang, Y. and Bau, H.H., 1997. "Thermoacoustic waves in a confined medium". *International Journal of Heat and Mass Transfer*, Vol. 40, No. 2, pp. 407–419.

Knupp, D., Naveira-Cotta, C. and Cotta, R.M., 2012. "Theoretical analysis of conjugated heat transfer with a single domain formulation and integral transforms". *International Communications in Heat and Mass Transfer*, Vol. 39, pp. 355–362.

Lima, J.A., Quaresma, J.N.N. and Macêdo, E.N., 2007. "Integral transform analysis of mhd flow and heat transfer in parallel-plates channels". *International Communications in Heat and Mass Transfer*, Vol. 34, pp. 420–431.

Mikhailov, M.D. and Özisik, M.N., 1984. *Unified Analysis and Solutions of Heat and Mass Diffusion*. John Wiley & Sons, New York.

Moler, C. and Loan, C.V., 2003. "Nineteen dubious ways to compute the exponential of a matrix, twenty-five years later". *SIAM Review*, Vol. 45, No. 1, pp. 1–46.

Nitsche, K. and Straub, J., 1987. "The critical hump of cv under microgravity, results from d-spacelab experiment". In *Proceedings of the 6th European Symposium on Material Sciences under Microgravity Conditions*. ESA SP-256.

Onuki, A. and Ferrell, R.A., 1990. "Adiabatic heating effect near the gas-liquid critical point". *Physica A*, Vol. 164, pp. 245–264.

Onuki, A., Hao, H. and Ferrell, R.A., 1990. "Fast adiabatic equilibration in a single-component fluid near the liquid-vapor critical point". *Physical Review A*, Vol. 41, No. 4, pp. 2256–2259.

Özisik, M.N., 1993. *Heat Conduction*. Wiley Interscience, New York, 2nd edition.

Schlichting, H., 1986. *Boundary-Layer Theory*. MacGraw Hill, Inc., New York, 7th edition.

Sphaier, L.A. and Cotta, R.M., 2002. "Analytical and hybrid solutions of diffusion problems within arbitrarily shaped regions via integral transforms". *Computational Mechanics*, Vol. 29, No. 3, pp. 265–276.

Wolfram, S., 2003. *The Mathematica Book*. Wolfram Media. Cambridge University Press, New York, 5th edition.

Zappoli, B., 2003. "Near-critical fluid hydrodynamics". *Comptes Rendus Mecanique*, Vol. 331, pp. 713–726.

Zappoli, B., Bailly, D., Garrabos, Y., Neindre, B.L., Guenoun, P. and Beysens, D., 1990. "Anomalous heat transport by the piston effect in supercritical fluids under zero gravity". *Physical Review A*, Vol. 41, No. 4, pp. 2264–2267.

7. RESPONSIBILITY NOTICE

The author is the only responsible for the printed material included in this paper.